# Measurement of the branching fractions for $B \to \omega K$ and $B \to \omega \pi$

C. H. Wang,[21] K. Abe,[6] K. Abe,[37] N. Abe,[40] T. Abe,[6] I. Adachi,[6] H. Aihara,[39] M. Akatsu,[19] T. Aso,[43] V. Aulchenko,[1] T. Aushev,[10] S. Bahinipati,[3] A. M. Bakich,[34] Y. Ban,[29] S. Banerjee,[35] S. Blyth,[22] A. Bondar,[1] A. Bozek,[23] M. Bračko,[17,11] T. E. Browder,[5] Y. Chao,[22] K.-F. Chen,[22] B. G. Cheon,[33] R. Chistov,[10] S.-K. Choi,[4] Y. Choi,[33] A. Chuvikov,[30] S. Cole,[34] M. Danilov,[10] L. Y. Dong,[8] S. Eidelman,[1] V. Eiges,[10] T. Gershon,[6] B. Golob,[16,11] J. Haba,[6] N. C. Hastings,[6] H. Hayashii,[20] M. Hazumi,[6] L. Hinz,[15] T. Hokuue,[19] Y. Hoshi,[37] W.-S. Hou,[22] Y. B. Hsiung,[22,*] H.-C. Huang,[22] T. Iijima,[19] K. Inami,[19] A. Ishikawa,[6] R. Itoh,[6] H. Iwasaki,[6] M. Iwasaki,[39] J. H. Kang,[47] J. S. Kang,[13] P. Kapusta,[23] N. Katayama,[6] H. Kawai,[2] T. Kawasaki,[25] H. Kichimi,[6] H. J. Kim,[47] J. H. Kim,[33] S. K. Kim,[32] P. Koppenburg,[6] S. Korpar,[17,11] P. Križan,[16,11] P. Krokovny,[1] Y.-J. Kwon,[47] G. Leder,[9] S. H. Lee,[32] T. Lesiak,[23] J. Li,[31] A. Limosani,[18] S.-W. Lin,[22] D. Liventsev,[10] J. MacNaughton,[9] G. Majumder,[35] F. Mandl,[9] T. Matsumoto,[41] W. Mitaroff,[9] K. Miyabayashi,[20] H. Miyata,[25] D. Mohapatra,[45] G. R. Moloney,[18] T. Mori,[40] T. Nagamine,[38] Y. Nagasaka,[7] E. Nakano,[26] M. Nakao,[6] Z. Natkaniec,[23] S. Nishida,[6] O. Nitoh,[42] S. Ogawa,[36] T. Ohshima,[19] T. Okabe,[19] S. Okuno,[12] S. L. Olsen,[5] W. Ostrowicz,[23] H. Ozaki,[6] H. Palka,[23] C. W. Park,[13] H. Park,[14] N. Parslow,[34] L. E. Piilonen,[45] A. Poluektov,[1] M. Rozanska,[23] H. Sagawa,[6] Y. Sakai,[6] O. Schneider,[15] J. Schümann,[22] S. Semenov,[10] K. Senyo,[19] V. Sidorov,[1] J. B. Singh,[28] N. Soni,[28] R. Stamen,[6] S. Stanič,[44,†] M. Starič,[11] K. Sumisawa,[27] T. Sumiyoshi,[41] S. Suzuki,[46] O. Tajima,[38] F. Takasaki,[6] N. Tamura,[25] M. Tanaka,[6] Y. Teramoto,[26] T. Tomura,[39] T. Tsukamoto,[6] S. Uehara,[6] K. Ueno,[2] T. Uglov,[10] S. Uno,[6] G. Varner,[5] C. C. Wang,[22] M.-Z. Wang,[22] Y. Watanabe,[40] B. D. Yabsley,[45] Y. Yamada,[6] A. Yamaguchi,[38] Y. Yamashita,[24] M. Yamauchi,[6] H. Yanai,[25] J. Ying,[29] Y. Yusa,[38] C. C. Zhang,[8] Z. P. Zhang,[31] and D. Žontar[16,11]

(Belle Collaboration)

[1]*Budker Institute of Nuclear Physics, Novosibirsk*
[2]*Chiba University, Chiba*
[3]*University of Cincinnati, Cincinnati, Ohio 45221*
[4]*Gyeongsang National University, Chinju*
[5]*University of Hawaii, Honolulu, Hawaii 96822*
[6]*High Energy Accelerator Research Organization (KEK), Tsukuba*
[7]*Hiroshima Institute of Technology, Hiroshima*
[8]*Institute of High Energy Physics, Chinese Academy of Sciences, Beijing*
[9]*Institute of High Energy Physics, Vienna*
[10]*Institute for Theoretical and Experimental Physics, Moscow*
[11]*J. Stefan Institute, Ljubljana*
[12]*Kanagawa University, Yokohama*
[13]*Korea University, Seoul*
[14]*Kyungpook National University, Taegu*
[15]*Swiss Federal Institute of Technology of Lausanne, EPFL, Lausanne*
[16]*University of Ljubljana, Ljubljana*
[17]*University of Maribor, Maribor*
[18]*University of Melbourne, Victoria*
[19]*Nagoya University, Nagoya*
[20]*Nara Women's University, Nara*
[21]*National United University, Miao Li*
[22]*Department of Physics, National Taiwan University, Taipei*
[23]*H. Niewodniczanski Institute of Nuclear Physics, Krakow*
[24]*Nihon Dental College, Niigata*
[25]*Niigata University, Niigata*
[26]*Osaka City University, Osaka*
[27]*Osaka University, Osaka*
[28]*Panjab University, Chandigarh*
[29]*Peking University, Beijing*
[30]*Princeton University, Princeton, New Jersey 08545*
[31]*University of Science and Technology of China, Hefei*
[32]*Seoul National University, Seoul*
[33]*Sungkyunkwan University, Suwon*
[34]*University of Sydney, Sydney NSW*
[35]*Tata Institute of Fundamental Research, Bombay*
[36]*Toho University, Funabashi*
[37]*Tohoku Gakuin University, Tagajo*
[38]*Tohoku University, Sendai*

 

[39]*Department of Physics, University of Tokyo, Tokyo*
[40]*Tokyo Institute of Technology, Tokyo*
[41]*Tokyo Metropolitan University, Tokyo*
[42]*Tokyo University of Agriculture and Technology, Tokyo*
[43]*Toyama National College of Maritime Technology, Toyama*
[44]*University of Tsukuba, Tsukuba*
[45]*Virginia Polytechnic Institute and State University, Blacksburg, Virginia 24061*
[46]*Yokkaichi University, Yokkaichi*
[47]*Yonsei University, Seoul*

(Received 26 March 2004; published 19 July 2004)

We report improved measurements of branching fractions for charmless hadronic two-body $B$ meson decays containing an $\omega$ meson in the final state. The results are based on a data sample of 78 fb$^{-1}$ collected on the $\Upsilon(4S)$ resonance by the Belle detector. We measure the branching fractions $\mathcal{B}(B^+\to\omega K^+)=(6.5^{+1.3}_{-1.2}\pm 0.6)\times 10^{-6}$ and $\mathcal{B}(B^+\to\omega\pi^+)=(5.7^{+1.4}_{-1.3}\pm 0.6)\times 10^{-6}$. We give 90% confidence upper limits for $\mathcal{B}(B^0\to\omega K^0)<7.6\times 10^{-6}$ and $\mathcal{B}(B^0\to\omega\pi^0)<1.9\times 10^{-6}$. We also obtain the partial rate asymmetries $\mathcal{A}_{CP}=0.06^{+0.21}_{-0.18}\pm 0.01$ for $B^\pm\to\omega K^\pm$ and $\mathcal{A}_{CP}=0.50^{+0.23}_{-0.20}\pm 0.02$ for $B^\pm\to\omega\pi^\pm$.

DOI: 10.1103/PhysRevD.70.012001 PACS number(s): 13.25.Hw, 14.40.Nd

## I. INTRODUCTION

Charmless hadronic $B$ decays play an important role in the understanding of $CP$ violation in the $B$ system. These decays proceed primarily through interfering $b\to s$ loop penguin diagrams and $b\to u$ tree spectator diagrams. Studies of $B\to\omega h$, where $h$ denotes $K^+$, $\pi^+$, $K^0$, and $\pi^0$, are important examples of such decays. Charge conjugates are implied unless otherwise stated. We also assume equal production of $B^+B^-$ and $B^0\overline{B}^0$ pairs from the $\Upsilon(4S)$.

Table I lists the branching fractions from previous measurements [1–5], which indicate some discrepancies for $B^+\to\omega K^+$. Naive factorization and QCD factorization approaches [6,7] yield values of $\mathcal{B}(B^+\to\omega\pi^+)$ consistent with the experimental results. However, these approaches predict $\mathcal{B}(B^+\to\omega\pi^+)$ to be a factor of two larger than $\mathcal{B}(B^+\to\omega K^+)$, which is not supported by Belle's previous experimental results that were based on a 29.4 fb$^{-1}$ data sample [5]. In this paper, we update our previous measurements on $\omega K^+$ and $\omega\pi^+$ with a 78.1 fb$^{-1}$ data sample. We also report measurements of $\omega K^0$ and $\omega\pi^0$ decay modes.

## II. APPARATUS AND DATA SET

The data sample used was collected with the Belle detector at the KEKB asymmetric energy $e^+e^-$ collider [8], which collides 8.0 GeV $e^-$ and 3.5 GeV $e^+$ beams at a small crossing angle ($\pm 11$ mrad). The data sample contained $85.0\times 10^6$ $B\overline{B}$ pairs produced at the $\Upsilon(4S)$ resonance. A 8.8 fb$^{-1}$ data sample taken at a center-of-mass energy 60 MeV below the $\Upsilon(4S)$ is used to characterize continuum background. In order to establish the event selection criteria, we use a Monte Carlo (MC) generator [9] to generate signal, generic $b\to c$, and other charmless rare $B$ decays. The GEANT3 package [10] is used for detector simulation.

The Belle detector measures charged particles and photons with high efficiency and precision [11]. Charged particle tracking is provided by a silicon vertex detector (SVD) and a central drift chamber (CDC) that surround the interaction region. The charged particle acceptance covers the laboratory polar angle region between $\theta=17°$ and 150°. Charged hadrons are distinguished by combining the responses from an array of silica aerogel Cerenkov counters (ACC), a barrel-like array of 128 time-of-flight scintillation counters (TOF), and $dE/dx$ measurements in the CDC. The combined response provides $K/\pi$ separation of at least $2.5\sigma$ for laboratory momentum up to 3.5 GeV/$c$. Electromagnetic showers are detected in an array of 8736 CsI(Tl) crystals (ECL) located inside the magnetic volume, which covers the same solid angle as the charged particle tracking system. The magnet return yoke consists of alternating layers of resistive plate counters and 4.7 cm thick steel plates for detecting $K_L^0$'s and identifying muons.

## III. EVENT SELECTION

Hadronic events are selected using criteria based on the charged track multiplicity and total visible energy sum; the efficiency is greater than 99% for generic $B\overline{B}$ events [12]. All primary charged tracks must satisfy quality requirements based on their impact parameters relative to the run-dependent interaction point (IP). The deviation from the IP position is required to be within $\pm 1.5$ cm in the transverse direction and $\pm 2$ cm in the longitudinal direction. Charged

TABLE I. Measurements of branching fractions for $B^+\to\omega K^+$ and $B^+\to\omega\pi^+$ from CLEO, BaBar and Belle. The units are $10^{-6}$.

| Mode | CLEO [2] | BaBar [4] | Belle [5] |
|---|---|---|---|
| $\omega K^+$ | $3.2^{+2.4}_{-1.9}\pm 0.8$ | $5.5\pm 0.9\pm 0.5$ | $9.2^{+2.6}_{-2.3}\pm 1.0$ |
| $\omega\pi^+$ | $11.3^{+3.3}_{-2.9}\pm 1.4$ | $4.8\pm 0.8\pm 0.4$ | $4.2^{+2.0}_{-1.8}\pm 0.5$ |

*On leave from Fermi National Accelerator Laboratory, Batavia, Illinois 60510, USA.

†On leave from Nova Gorica Polytechnic, Nova Gorica.

particle identification is based on the ratio KID$=\mathcal{L}_K/(\mathcal{L}_\pi+\mathcal{L}_K)$, where $\mathcal{L}_K$ and $\mathcal{L}_\pi$ are likelihoods for $K$ and $\pi$ hypotheses. A higher value of KID indicates a more kaon-like particle. $\pi^0$ meson candidates are reconstructed from pairs of photons, each consisting of energy clusters greater than 50 MeV, with $\gamma\gamma$ invariant mass within $3\sigma$ ($\sigma=5.4$ MeV/$c^2$) of the $\pi^0$ mass. $K_S^0$ meson candidates are reconstructed using pairs of oppositely charged particles that have an invariant mass in the range 480 MeV/$c^2<m(\pi^+\pi^-)<516$ MeV/$c^2$. The vertex of the $K_S^0$ candidate is required to be well reconstructed and displaced from the interaction point, and the $K_S^0$ momentum direction must be consistent with the $K_S^0$ flight direction. Candidate $\omega\to\pi^+\pi^-\pi^0$ decays are reconstructed from charged pions with KID $<0.9$ and $\pi^0$s with center-of-mass frame momentum greater than 0.35 GeV/$c$. The $\omega$ meson candidates are required to have an invariant mass within $\pm 30$ MeV/$c^2$ of the nominal value ($\pm 2\sigma$).

## IV. *B* RECONSTRUCTION

*B* meson candidates are formed by combining an $\omega$ meson with either a kaon ($K^+$,$K^0$) or a pion ($\pi^+$,$\pi^0$). We require KID $>0.6$ and KID $<0.4$ for $K^+$ and $\pi^+$, respectively. Studies from $D^{*+}\to D^0\pi^+(D^0\to K^-\pi^+)$ decays give particle identification efficiencies, $\epsilon_K=85\%$ and $\epsilon_\pi=89\%$ with misidentification rates, $f_\pi=8\%$ and $f_K=11\%$, respectively.

*B* meson candidates are then identified using the beam constrained mass $M_{\rm bc}=\sqrt{(E_{\rm beam}^{\rm CM})^2-|P_B^{\rm CM}|^2}$ and the energy difference $\Delta E=E_B^{\rm CM}-E_{\rm beam}^{\rm CM}$, where $E_{\rm beam}^{\rm CM}=5.29$ GeV, and $P_B^{\rm CM}$, $E_B^{\rm CM}$ are the momentum and energy of the *B* candidate in the $\Upsilon(4S)$ rest frame. For the $\Delta E$ calculation, the kaon in candidate $B^+\to\omega K^+$ decays is assigned a pion mass so that $\omega K^+$ and $\omega\pi^+$ can be fit simultaneously. For events with multiple candidates, the best candidate is selected using the quality of the *B* vertex fit. According to signal MC, the resolutions for $M_{\rm bc}$ and $\Delta E$ are 3 MeV/$c^2$ and 24 MeV respectively for $B\to\omega K^+$, $\omega\pi^+$ and $\omega K^0$ decays. For the decay $B\to\omega\pi^0$, the resolutions are 3.5 MeV/$c^2$ for $M_{\rm bc}$ and 55 MeV for $\Delta E$.

The *B* candidates are required to be within the rectangular region in the $M_{\rm bc}-\Delta E$ plane, 5.2 GeV/$c^2<M_{\rm bc}<5.3$ GeV/$c^2$ and $|\Delta E|<0.25$ GeV. Signal regions of 5.27 GeV/$c^2<M_{\rm bc}<5.3$ GeV/$c^2$ and $|\Delta E|<0.10$ GeV are used to display fit projections. Sideband regions are defined as 5.2 GeV/$c^2<M_{\rm bc}<5.26$ GeV/$c^2$ with $|\Delta E|<0.25$ GeV for $\Delta E$, and 5.2 GeV/$c^2<M_{\rm bc}$ with 0.10 GeV$<|\Delta E|<0.25$ GeV for $M_{\rm bc}$.

Since $B\to\omega h$ is a $P\to VP$ decay, where $V$ means vector and $P$ means pseudoscalar particles, the $\omega$ meson is polarized. The $\omega$ helicity angle, $\theta_{\rm hel}$, is defined as the angle between the *B* flight direction and the vector perpendicular to the $\omega$ decay plane in the $\omega$ rest frame. Further background suppression is achieved using the $\omega$ helicity and the quality of the *B* vertex fit ($\chi_B^2$).

## V. BACKGROUND SUPPRESSION

Backgrounds from $b\to c$ decays and the feed-across from other charmless rare *B* decays are found to be negligible using MC simulations that assume the best known branching fraction for each decay. The dominant backgrounds arise from the $e^+e^-\to q\bar{q}$ ($q=u$, $d$, $s$ or $c$) continuum process, which has a jet-like event topology in contrast to the spherical $B\bar{B}$ events.

Several event-shape variables are used to distinguish between *B* decays and continuum background. The thrust angle $\theta_T$ is defined as the angle between the primary *B* decay daughter $\omega$ and the thrust axis formed by all the particles from the other *B*. $S_\perp$ is the scalar sum of the transverse momenta of all particles outside a 45° cone around the primary *B* decay daughter direction divided by the scalar sum of their momenta. In addition to these, a set of variables derived from Fox-Wolfram moments [13] are used. The moments are defined by

$$R_l^{so}=\frac{\sum_{i,k}|p_i||p_k|P_l(\cos\theta_{ik})}{\sum_{i,k}|p_i||p_k|},$$

and

$$R_l^{oo}=\frac{\sum_{i,j}|p_i||p_j|P_l(\cos\theta_{ij})}{\sum_{i,j}|p_i||p_j|},$$

where $p$ stands for particle momentum, and $P_l$ is the $l$th Legendre polynomial. There are two groups of particles that go into this summation. The index $k$ refers to (neutral or charged) particles from the *B* candidate, while $i$ and $j$ refer to other particles not from that *B* candidate. $R_1^{so}$, $R_3^{so}$ and $R_1^{oo}$ are not used because of their strong correlation with $M_{\rm bc}$. To optimize the discrimination, the remaining 5 variables ($l\leqslant 4$) are combined with $\cos\theta_T$ and $S_\perp$ to form a Fisher discriminant $\mathcal{F}$ [14,15]. The cosine of the angle between the *B* flight direction and the beam axis ($\cos\theta_B$), and $\mathcal{F}$ are found to be independent, and their probability density functions (PDFs) are obtained by using MC samples for signal, and off-resonance data for continuum background. The variables $\cos\theta_B$ and $\mathcal{F}$ are then combined to form a likelihood ratio $\mathcal{L}R=\mathcal{L}_s/(\mathcal{L}_s+\mathcal{L}_{bg})$, where $\mathcal{L}_{s(bg)}$ is the product of signal ($q\bar{q}$) PDFs. A selection requirement is imposed on $\mathcal{L}R$ to reject continuum background. A typical cut is $\mathcal{L}R>0.5$ and retains approximately 83% of the signal candidates while reducing the background by approximately 73%.

## VI. ANALYSIS

Signal yields are obtained using $M_{\rm bc}$ and $\Delta E$ as independent variables in an extended unbinned maximum likelihood (ML) fit after restrictions are imposed on the variables $\chi_B^2$, $\mathcal{L}R$ and $\cos\theta_{\rm hel}$. These are $\mathcal{L}R>0.65$ for $\omega K^+/\pi^+$, $\mathcal{L}R>0.5$ for $\omega K^0$, $\mathcal{L}R>0.8$ for $\omega\pi^0$ and $|\cos\theta_{\rm hel}|>0.5$. For $N$ input candidates, the likelihood is defined as

TABLE II. Signal yields ($N_s$), efficiencies ($\epsilon_{tot}$) including secondary decay branching fractions, fit significances ($\Sigma$), branching fractions ($\mathcal{B}$), and 90% confidence level upper limits (UL) on the branching fractions for $\omega K^0$ and $\omega\pi^0$.

| Mode | $N_s$ | $\epsilon_{tot}(\%)$ | $\Sigma$ | $\mathcal{B}$ ($\times 10^{-6}$) | UL ($\times 10^{-6}$) |
|---|---|---|---|---|---|
| $\omega K^+$ | $44.6^{+9.1}_{-8.3}$ | 8.1 | $7.8\sigma$ | $6.5^{+1.3}_{-1.2}\pm 0.6$ | |
| $\omega\pi^+$ | $42.1^{+10.1}_{-9.3}$ | 8.7 | $6.0\sigma$ | $5.7^{+1.4}_{-1.3}\pm 0.6$ | |
| $\omega K^0$ | $11.1^{+5.2}_{-4.4}$ | 3.3 | $3.2\sigma$ | $4.0^{+1.9}_{-1.6}\pm 0.5$ | 7.6 |
| $\omega\pi^0$ | $0^{+2.1}_{-0.0}$ | 5.2 | | | 1.9 |

$$\mathcal{L}(N_S,N_B)=e^{-(N_S+N_B)}\prod_{i=1}^{N}[N_S P_{S_i}(M_{\rm bc})P_{S_i}(\Delta E) + N_B P_{B_i}(M_{\rm bc})P_{B_i}(\Delta E)],$$

where the index $i$ runs over each event, and $P_{S_i}$ and $P_{B_i}$ are the probability densities as functions of $M_{\rm bc}$ and $\Delta E$ for signal and background, respectively. This method treats the extracted yields for signal $N_S$ and background $N_B$ according to Poisson statistics and constrains their sum to the observed number of candidates $N$ at the maximum likelihood.

The signal PDFs are determined from signal MC while the continuum background PDFs are derived from the off-resonance data. The background shapes are verified using data from the sideband region. The PDF for the $\Delta E$ background is modeled by a second-order polynomial function. The PDF for the $M_{\rm bc}$ background distribution is modeled with a smooth function with parameters determined from off-resonance data [16]. To model the low energy tail, the $\Delta E$ signal PDFs use a "Crystal Ball" line shape function [17] with parameters determined by fits to signal MC. The $M_{\rm bc}$ PDFs are the sum of two Gaussian functions with different widths, which were obtained by fits to signal MC. Studies of $B^+\to\bar{D}^0\pi^+$ and $\bar{D}^0\to K^+\pi^-\pi^0$ decays were used to fix the mean $M_{\rm bc}$. Differences between widths obtained in these studies and those from the signal MC are regarded as systematic uncertainties.

The overall reconstruction efficiencies, $\epsilon$, are the products of detection efficiencies, determined from MC with no KID requirements, and KID efficiencies determined from $D^{*+}\to D^0\pi^+$, $D^0\to K^-\pi^+$ events in the data. The statistical significance ($\Sigma$) is defined as $\sqrt{-2\ln[\mathcal{L}(0)/\mathcal{L}_{\rm max}]}$, where $\mathcal{L}_{\rm max}$ is the maximum likelihood at the nominal signal yield and $\mathcal{L}(0)$ is the likelihood with the signal fixed at zero. The 90% confidence level upper limit is calculated from the equation

$$\frac{\int_0^{x_{\rm max}}\mathcal{L}(x)dx}{\int_0^{\infty}\mathcal{L}(x)dx}=90\%,$$

where only the statistical uncertainties are considered. For the final upper limit, the above limit is increased by one standard deviation of the systematic error.

## VII. MEASUREMENTS OF BRANCHING FRACTIONS

The results from the fits are shown in Table II. Figure 1 shows the $M_{\rm bc}$ and $\Delta E$ distributions, where events in the $M_{\rm bc}$ ($\Delta E$) plots are required to be in the $\Delta E$ ($M_{\rm bc}$) signal region after all selection criteria. The signal yields from the fits are $N_{\omega K^+}=44.6^{+9.1}_{-8.3}$, $N_{\omega\pi^+}=42.1^{+10.1}_{-9.3}$ and $N_{\omega K^0}=11.1^{+5.2}_{-4.4}$ (statistical errors only). No signal is observed for $B^0\to\omega\pi^0$. For $B^+\to\omega\pi^+$ and $\omega K^+$, the $\pi^+/K^+$ feed-across is not negligible and its level is fixed in the ML fit. For $B^+\to\omega\pi^+$, the contribution is estimated by using $\omega K^+$ yields from the fitted $B^+\to\omega K^+$ candidate events assuming no feed-across from $\omega\pi^+$, dividing by the kaon efficiency and multiplying by the kaon misidentification probability. The result is $4.8\pm 1.0$ events from $B^+\to\omega K^+$ in the $B^+\to\omega\pi^+$ signal. This value is consistent with the level determined by repeating the fit for $B^+\to\omega\pi^+$ with the level of $\omega K^+$ feed-across left as a free parameter: $11.6\pm 9.0$ events. This difference is assigned to the systematic error of $\omega K^+$ feed-across for $\omega\pi^+$ decay. A

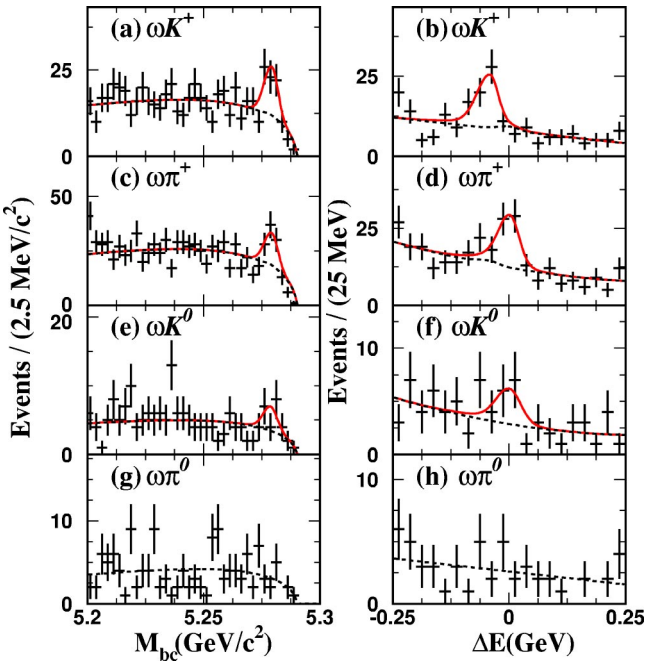


FIG. 1. Signal region projections of $M_{\rm bc}$ (left) and $\Delta E$ (right) for $\omega K^+$, $\omega\pi^+$, $\omega K^0$ and $\omega\pi^0$. The solid curves show the results of the 2D fits with the background components represented as dashed curves. Small background enhancements near 0 MeV in (b) and $-50$ MeV in (d) are from misidentified $B^+\to\omega\pi^+$ and $B^+\to\omega K^+$ decays.

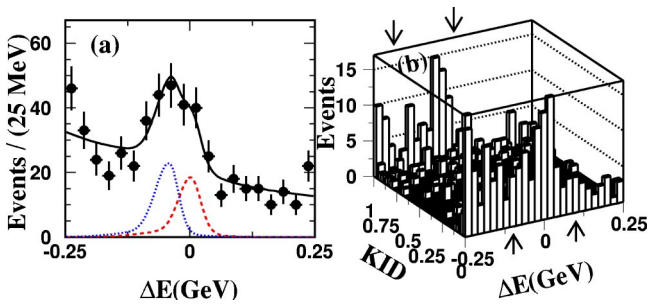


FIG. 2. (a) $\Delta E$ distributions without KID requirements in the $M_{\rm bc}$ signal region. Dotted (dashed) curves indicate the signal components $\omega K^+$ ($\omega\pi^+$) obtained from the $\Delta E$ fit to the $B^+\to\omega h^+$ candidate events. The solid curve shows the sum of signal and continuum background components. (b) KID vs $\Delta E$ distributions in the $M_{\rm bc}$ signal region. Arrows show the signal $\Delta E$ region with $KID>0.6$ for $\omega K^+$ and $KID<0.4$ for $\omega\pi^+$.

similar procedure is used to determine the $\omega\pi^+$ contamination in the $B^+\to\omega K^+$ yield. Here the feed-across is found to be $3.3\pm0.7$ events. The final measurements of branching fractions are listed in Table II.

Because of the assignment of the pion mass to the kaon, the $B^+\to\omega K^+$ signal peaks at $\Delta E=-50$ MeV, which provides some discrimination from $B^+\to\omega\pi^+$ events, which peak at $\Delta E=0$ MeV. We use this to provide a consistency check of the $\omega K^+$ and $\omega\pi^+$ yields by fitting to the $\Delta E$ distribution for $B^+\to\omega h^+$ candidates with no KID requirements applied. The signal yields are $60.0^{+15.5}_{-14.8}$ and $47.7^{+14.6}_{-13.7}$ events for $\omega K^+$ and $\omega\pi^+$, respectively, which are consistent with the results using the KID, where the efficiency-corrected yields are $52.4^{+10.7}_{-9.8}$ events for $\omega K^+$ and $47.3^{+11.3}_{-11.0}$ events for $\omega\pi^+$. Figure 2 shows the results of this fit and a lego plot of KID versus $\Delta E$. From the lego plot, there is a clear separation in the KID distribution between $\omega K^+$ and $\omega\pi^+$ signal yields, which also provides a consistency check.

We also examine the properties of $\omega$ candidates in our fit sample. The clear $\omega$ mass peak and polarized $\cos\theta_{\rm hel}$ distribution shown in Figs. 3(a) and 3(b) confirm our fitted signals are from $\omega$ mesons with no significant nonresonant $\pi^+\pi^-\pi^0$ contribution. Several other consistency checks have also been performed including tightening $\mathcal{L}R$ requirements and performing 1D ML fits to $M_{\rm bc}$ and $\Delta E$. All studies yield consistent results.

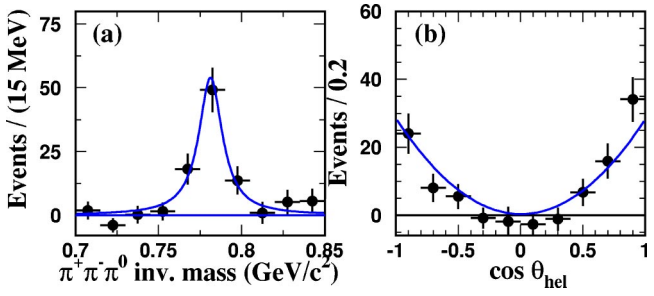


FIG. 3. Fitted yields in bins of (a) $\pi^+\pi^-\pi^0$ invariant mass and (b) cosine of $\omega$ helicity angle for $\omega K^+$ and $\omega\pi^+$. Solid curves show the distribution from signal MC normalized to the results from the fits.

TABLE III. Systematic errors for $\omega h$. Feed-across means $\omega K^+(\pi^+)$ for $\omega\pi^+(K^+)$ decay. The unit is in percent (%).

| Mode | $\omega K^+$ | $\omega\pi^+$ | $\omega K^0$ | $\omega\pi^0$ |
|---|---|---|---|---|
| Background suppression | 4.4 | 4.4 | 4.4 | 4.4 |
| Reconstruction | 8.0 | 8.0 | 9.5 | 9.4 |
| Fit | $^{+1.3}_{-1.6}$ | $^{+1.6}_{-1.8}$ | $^{+4.4}_{-4.3}$ | |
| Feed-across | $\pm1.6$ | $^{+3.6}_{-3.3}$ | | |
| $N_{B\bar{B}}$ | 1 | 1 | 1 | 1 |
| $\mathcal{B}(\omega\to\pi^+\pi^-\pi^0)$ | 0.8 | 0.8 | 0.8 | 0.8 |
| Sum | 9.4 | 10.0 | 11.4 | 10.6 |

Systematic uncertainties for each mode are presented in Table III, with contributions arising from the background suppression, reconstruction and the fitting function variations. The systematic errors from the MC modeling of the $\chi^2_B$ and $\mathcal{L}R$ requirements are studied with $B^+\to\bar{D}^0\pi^+$ and $\bar{D}^0\to K^+\pi^-\pi^0$ decays, which are 2.0% for $\mathcal{L}R$ and 3.0% for $\chi^2_B$. We study the systematic error associated with the $\omega$ polarization ($\cos\theta_{\rm hel}$) requirement $|\cos\theta_{\rm hel}|<0.5$ by comparing the MC distributions with the fitted yields distribution (Fig. 3). We assign a 2.6% systematic error. The total systematic error from background suppression is 4.4%. The systematic error due to uncertainties in the reconstruction is determined from detailed studies of the charged particle tracking, $\omega$ mass resolution, KID and $\pi^0$ detection. For charged tracking and $\pi^0$ detection, the decay modes $\eta\to\gamma\gamma,\pi^+\pi^-\pi^0$ and $\eta\to\pi^0\pi^0\pi^0$ are used. By comparing results in data and MC, we assign a relative error of 2.0% for charged track reconstruction, 3.0% for $\omega$ mass cut, and 4% for $\pi^0$ detection. The total reconstruction systematic error ranges between 8.0% and 9.5%. The mean and width differences of $M_{\rm bc}$ and $\Delta E$ distributions between data and MC from $B^+\to\bar{D}^0\pi^+$ decays are included in the systematic errors from fitting. The systematic uncertainty on the branching fraction of $\omega\to\pi^+\pi^-\pi^0$ is obtained from the PDG tables [18].

## VIII. $\mathcal{A}_{CP}$ MEASUREMENTS

We determine partial rate asymmetries defined as

$$\mathcal{A}_{CP}=\frac{N(B^-\to\omega h^-)-N(B^+\to\omega h^+)}{N(B^-\to\omega h^-)+N(B^+\to\omega h^+)}.$$

The values of $\mathcal{A}_{CP}$ were measured for the modes $B^\pm\to\omega K^\pm$ and $B^\pm\to\omega\pi^\pm$ by performing 2D $M_{\rm bc}-\Delta E$ fits to the $B^+$ and $B^-$ separately, as shown in Fig. 4. The number of signal events in the $\omega K^\pm$ and $\omega\pi^\pm$ modes are $21.0^{+6.4}_{-5.7}$, and $10.7^{+6.1}_{-5.2}$ for $B^+$ decays, and $23.6^{+6.6}_{-5.9}$ and $32.2^{+8.2}_{-7.4}$ for $B^-$ decays, respectively. The corresponding partial rate asymmetry values are $\mathcal{A}_{CP}=0.06^{+0.21}_{-0.18}\pm0.01$ for $\omega K^\pm$ and $\mathcal{A}_{CP}=0.50^{+0.23}_{-0.20}\pm0.02$ for $\omega\pi^\pm$. The systematic error in $\mathcal{A}_{CP}$ comes mainly from the reconstruction efficiency of high momentum charged particles and the fitting functions. The latter is measured by varying the parameters of the fitting functions. The asymmetry in $K^\pm$ reconstruction efficiency is studied with an inclusive charged kaon sample.

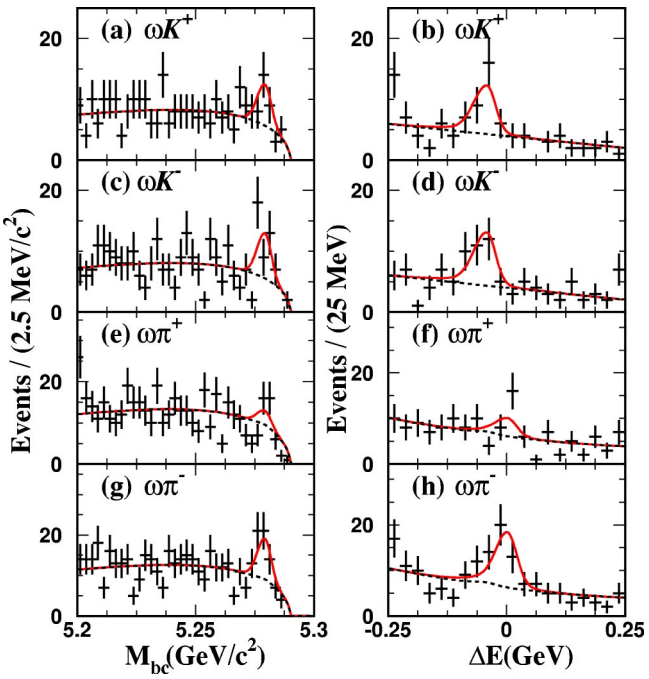


FIG. 4. Projections of the 2D $M_{\rm bc}$ and $\Delta E$ for $B^{\pm}\to\omega K^{\pm}$ and $B^{\pm}\to\omega\pi^{\pm}$ decays. Solid curves show the fit results. The dashed curves indicate the backgrounds.

In the confidence level calculation, we expand the interval determined solely from the statistical error by one standard deviation of the systematic error. The 90% confidence level interval corresponds to $-0.25<\mathcal{A}_{CP}<0.41$ for $B^{\pm}\to\omega K^{\pm}$ and $0.15<\mathcal{A}_{CP}<0.90$ for $B^{\pm}\to\omega\pi^{\pm}$.

## IX. DISCUSSION AND CONCLUSION

In summary, we have searched for exclusive two-body charmless hadronic $B$ decays with an $\omega$ meson in the final state using a data sample of 78.1 fb$^{-1}$ collected on the $\Upsilon(4S)$ resonance. We find $\mathcal{B}(B^+\to\omega K^+)=(6.5^{+1.3}_{-1.2}\pm0.6)\times10^{-6}$ and $\mathcal{B}(B^+\to\omega\pi^+)=(5.7^{+1.4}_{-1.3}\pm0.6)\times10^{-6}$, where the first error is statistical and the second systematic. Our results confirm our previous measurement of a large branching fractions for $B^+\to\omega K^+$, which cannot be easily accommodated by the factorization approach and might indicate the presence of a large nonfactorizable contribution or other penguin related processes [19]. A signal is obtained for $B^0\to\omega K^0$ decay with $3.2\sigma$ significance while no excess is observed for $B^0\to\omega\pi^0$ decay. The results correspond to 90% confidence level upper limits of $\mathcal{B}(B^0\to\omega K^0)<7.6\times10^{-6}$ and $\mathcal{B}(B^0\to\omega\pi^0)<1.9\times10^{-6}$.

We also search for partial rate asymmetries in $B^{\pm}\to\omega K^{\pm}$ and $\omega\pi^{\pm}$. We find $\mathcal{A}_{CP}=0.06^{+0.21}_{-0.18}\pm0.01$ for $\omega K^{\pm}$ and $\mathcal{A}_{CP}=0.50^{+0.23}_{-0.20}\pm0.02$ for $\omega\pi^{\pm}$. These correspond to 90% confidence level intervals of $-0.25<\mathcal{A}_{CP}<0.41$ for $B^{\pm}\to\omega K^{\pm}$ and $0.15<\mathcal{A}_{CP}<0.90$ for $B^{\pm}\to\omega\pi^{\pm}$. Our results indicate the possibility of nonzero $\mathcal{A}_{CP}$ for $B^{\pm}\to\omega\pi^{\pm}$ with 99.2% confidence level, equivalent to $2.4\sigma$ significance for Gaussian errors.

## ACKNOWLEDGMENTS

We wish to thank the KEKB accelerator group for the excellent operation of the KEKB accelerator. We acknowledge support from the Ministry of Education, Culture, Sports, Science, and Technology of Japan and the Japan Society for the Promotion of Science; the Australian Research Council and the Australian Department of Education, Science and Training; the National Science Foundation of China under contract No. 10175071; the Department of Science and Technology of India; the BK21 program of the Ministry of Education of Korea and the CHEP SRC program of the Korea Science and Engineering Foundation; the Polish State Committee for Scientific Research under contract No. 2P03B 01324; the Ministry of Science and Technology of the Russian Federation; the Ministry of Education, Science and Sport of the Republic of Slovenia; the National Science Council and the Ministry of Education of Taiwan; and the U.S. Department of Energy.

[1] CLEO Collaboration, T. Bergfeld *et al.*, Phys. Rev. Lett. **81**, 272 (1998).
[2] CLEO Collaboration, C.P. Jessop *et al.*, Phys. Rev. Lett. **85**, 2881 (2000).
[3] BABAR Collaboration, B. Aubert *et al.*, Phys. Rev. Lett. **87**, 221802 (2001).
[4] BABAR Collaboration, B. Aubert *et al.*, Phys. Rev. Lett. **92**, 061801 (2004).
[5] Belle Collaboration, R.S. Lu *et al.*, Phys. Rev. Lett. **89**, 191801 (2002).
[6] A. Ali, G. Kramer, and C.D. Lu, Phys. Rev. D **58**, 094009 (1998); Y.H. Chen, H.Y. Cheng, B. Tseng, and K.C. Yang, *ibid.* **60**, 094014 (1999).
[7] D.S. Du, H.J. Gong, J.F. Sun, and G.H. Zhu, Phys. Rev. D **65**, 094025 (2002); C.D. Lu and M.Z. Yang, Eur. Phys. J. C **23**, 275 (2002).
[8] S. Kurokawa and E. Kikutani, Nucl. Instrum. Methods Phys. Res. A **499**, 1 (2003).
[9] The QQ B meson decay event generator was developed by the CLEO Collaboration.
[10] R. Brun *et al.*, GEANT 3.21, CERN Report DD/EE/84-1, 1984.
[11] Belle Collaboration, K. Abashian *et al.*, Nucl. Instrum. Methods Phys. Res. A **479**, 117 (2002).
[12] Belle Collaboration, K. Abe *et al.*, Phys. Rev. D **64**, 072001 (2001).
[13] G. Fox and S. Wolfram, Phys. Rev. Lett. **41**, 1581 (1978).
[14] R.A. Fisher, Ann. Eugenics. **7**, 179 (1936).
[15] K. Abe *et al.*, Phys. Lett. B **517**, 309 (2001).
[16] H. Albrecht *et al.*, Phys. Lett. B **241**, 278 (1990).
[17] J.E. Gaiser *et al.*, Phys. Rev. D **34**, 711 (1986).
[18] Particle Data Group, K. Hagiwara *et al.*, Phys. Rev. D **66**, 010001 (2002).
[19] R. Aleksan *et al.*, Phys. Rev. D **67**, 094019 (2003).